

United Nations Educational, Scientific and Cultural Organization
and
International Atomic Energy Agency

THE ABDUS SALAM INTERNATIONAL CENTRE FOR THEORETICAL PHYSICS

**DEPOSITION OF SINGLE-PHASE Cu(In,Ga)Se₂ THIN
FILMS FROM THE SELENIZATION OF THERMALLY
EVAPORATED InSe/Cu/GaSe PRECURSORS**

F.B. Dejene¹

*Department of Physics, University of the Free State, Phuthaditjhaba 9866, South Africa
and
The Abdus Salam International Centre for Theoretical Physics, Trieste, Italy.*

Abstract

The relatively small band gap values ($\sim 1\text{eV}$) of CuInSe₂ thin films limits the conversion efficiencies of completed CuInSe₂/CdS/ZnO solar cell devices. In the case of traditional two-stage growth techniques, limited success has been achieved to homogeneously increase the band gap by substituting indium with gallium. In this study, thermal evaporation of InSe/Cu/GaSe precursors were exposed to an elemental Se vapour under defined conditions. This technique produced large-grained, single-phase Cu(In,Ga)Se₂ thin films with a high degree of in-depth compositional uniformity. The selenization temperature, ramp time, reaction period and the effusion cell temperature with respect to the Cu(In,Ga)Se₂ films were optimized in this study. The homogeneous incorporation of Ga into CuInSe₂ led to a systematic shift in the lattice spacing parameters and band gap of the absorber films. Under optimized conditions, gallium in-cooperation resulted only in a marginal decrease in the grain size, X-ray diffraction studies confirmed single-phase Cu(In,Ga)Se₂ material and X-ray photoluminescence spectroscopy in-depth profiling revealed a uniform distribution of the elements through the entire depth of the alloy. From these studies optimum selenization conditions were determined for the deposition of homogeneous Cu(In,Ga)Se₂ thin films with optimum band gap values between 1.01 and 1.21 eV.

MIRAMARE – TRIESTE

March 2010

¹ Regular Associate of ICTP.

1. Introduction

CuInSe₂ (CIS) based thin film module technology is the candidate with best chances to compete with crystalline silicon. CuInSe₂ has a band gap of about 1.0 eV, which limits the conversion efficiency of complete CuInSe₂/CdS/ZnO devices. In order to increase the conversion efficiency of devices, it is necessary to increase the band gap value of the absorber films. This can be achieved by systematically substituting some indium with a group III element, such as gallium and/or selenium, with another group VI element such as sulphur. The substitution of In with Ga and/or Se with S results in the shrinkage of the *lattice parameters* and thus an increase in the band gap [1]. The conversion efficiencies of polycrystalline thin film solar cells based on Cu(In,Ga)Se₂ (CIGS) have already reached values above 19% at the laboratory scale [2]. The absorber films of these high efficiency devices are produced using a single-stage technique in which all the elements (Cu, In, Ga and Se) are co-evaporated from individual sources. This technique allows a controlled introduction of Ga into the structure and hence formation of single-phase material. In general, two-stage processing of thin chalcopyrite films uses techniques that are relatively easy to scale up in order to produce uniform coatings of thin films on large area substrates. The strength of two-stage approaches arises from the fact that they utilize various deposition techniques (sputtering, thermal evaporation, screen printing, and so on) in the precursor stage. During the subsequent reaction step, the precursors are exposed to either elemental Se in vapour or to H₂Se/Ar gas at atmospheric pressure [3, 4]. However, the efficiencies of Cu(In,Ga)Se₂/CdS/ZnO solar cell devices, in which the absorbers are produced using classical two-step processes, are in general significantly lower than those in which co-evaporated absorber films are used [5]. A significant problem related to the two-step growth process is the reported segregation of Ga towards the Mo back contact, resulting in separated CuInSe₂ and CuGaSe₂ phases [6-11]. As a result, these layers are normally completely depleted of Ga in the near surface region of the absorber film, and the characteristics of completed solar cell devices are similar to those of devices produced from pure CuInSe₂ absorber layers. In this study, we present experimental evidence that the diffusion of gallium towards the Mo back contact can be prevented in an optimized two-step growth process. The structural features of the homogeneous absorber layers are discussed and optical data are presented to illustrate the influence of the gallium in cooperation on the optical band gap of the semiconductor thin films.

2. Experimental details

2.1. Absorber formation

All films were deposited on Mo-coated soda-lime glass substrates. The Mo back contact was about 1µm thick and was deposited by electron beam evaporation. Selenium-containing precursors, InSe/Cu/GaSe were prepared by the sequential thermal evaporation of the respective elements from three separate graphite heaters. The temperatures of the graphite heaters were controlled carefully in order to maintain low growth rates of around 0.1 nms⁻¹. The thicknesses of the individual layers (~1200 nm InSe/180 nm Cu/~200 nm GaSe) and evaporation rates were measured with a quartz crystal monitor. The relative thickness of InSe with respect to GaSe was varied in order to vary the Ga/(Ga+In) ratio from 0 to 0.35, while keeping constant the Cu/Ga+In ratio at approximately 0.8. The substrate temperature was kept constant at 200°C and the deposition pressure was maintained at 10⁻⁵ mbar. More details about this process can be found elsewhere [12]. In the second step of the process, these stacked layers were reacted in vacuum to elemental Se vapour at 550°C for at least 60 min. In

all cases the substrate temperature was raised in 10 min from ambient to 550 °C. In order to ensure a uniform Se vapour flux during the selenization process, a stainless steel effusion cell was used, which was also raised from ambient temperature to 330 °C in 10 min.

2.2. Characterization

The surface morphologies were examined by scanning electron microscopy (SEM) and the crystalline structure of the films was evaluated with normal incidence x-ray diffraction (XRD) using Cu K α (0.15407 nm) radiation. The bulk compositional values of the precursors and reacted absorber layers were calculated from electron microprobe analysis (EMPA) at 20 kV. The optical measurements were carried out with a Carry UV-VIS-NIR spectrophotometer in the wavelength range 300 – 2000 nm. The in-depth compositional analyses of the samples were studied with x-ray photoelectron spectroscopy (XPS).

3. Results

3.1. Morphological properties

The ultimate aim of this study was to develop a relatively simple deposition process for the preparation of single phase Cu(In,Ga)Se₂ thin films with favourable material properties. It is well known that the final surface morphology of a specific sample is significantly influenced by the overall bulk composition of the film. Therefore, for the purpose of comparison, the precursors had similar bulk composition properties with (Cu/Ga+In) ratios of approximately 0.8. Figure 1(a) is a SEM micrograph of the typical surface morphology of the reference InSe/Cu/GaSe precursor before selenization, deposited by thermal evaporation at 200°C. The SEM micrograph was dominated by the presence of high density of mostly rounded grain with sizes that varied between 0.5 and 1 μ m. The reaction of these precursor films, with elemental Se vapour at 550°C for 60 min, resulted in the formation of densely packed, faceted chalcopyrite grains with typical sizes around 1 μ m. SEM studies (see figure 1(b)) clearly revealed the columnar growth structure of the grains, which is typical for device quality material. All of the selenized films exhibited good adherence to Mo/glass substrate. The typical thickness of the final Cu(In,Ga)Se₂ films was 2.5 μ m. It was anticipated that the crystalline quality of the Cu(In_{1-x}Ga_x)Se₂ thin films would be critically influenced by the Ga concentration in the bulk of the thin films (i.e. the value of x). For the purpose of comparison, films were prepared in which the value of x was varied between 0 and 0.35. It is important to note that an increase in gallium concentration resulted in a significant decrease in the average grain size of the film. This observation is in good agreement with other related studies [13-15].

3.2. Structural properties

Figure 2 (a) depicts XRD patterns of the precursor and selenized thin films with different gallium incorporations (x= 0.02, 0.22 and 0.35). The presence of the characteristic (112) diffraction peak of the chalcopyrite lattice in the precursor micrograph, is indicative of the partial formation of CuInSe₂ due to an inter-diffusion between Cu-selenide and In-selenide binary phases. The superior structural properties of the reference Cu(InGa)Se₂ film (see figure 1(b)) are clearly reflected by the XRD results in figure 2(a). All the major peaks in the XRD patterns of Cu(In,Ga)Se₂ thin films could be attributed to CuIn_{1-x}Ga_xSe₂ phases indicating principally the formation of homogeneous single phase. It is also important to note from figure 2(a) that selenization for 60 min, under the specific experimental conditions, resulted in

a fully reacted alloy with no evidence of binary phases (CuSe and InSe). Homogeneous and single-phase quaternary films are considered to be suitable for materials for high efficiency CIGS-based solar cells. These results are slightly different from those reported for the selenization of Cu-In-Ga precursors, where In tended to diffuse toward the surface and Ga toward the substrate, giving rise to phase separation into CIS and CGS [6–11]. As expected, an increase in gallium concentration resulted in shifts in 2θ angles. The Mo peak, which is clearly labeled, correspond fairly well (around $2\theta=40.5$) is used as correspondence in the various scans, while the shift in the chalcopyrite peaks attributed to the incorporation of more Ga can be observed. The insignificant deviation in the position of the Mo peaks is due to a very small difference in sample orientation during measurement. The positions of [116/312] diffraction peaks for the respective samples, shown in Fig. 2(b), clearly indicate a shift to higher diffraction angles due to the decrease in lattice parameters with increasing gallium concentration. This behavior is related to the fact that gallium atoms are smaller than indium atoms and hence causes the shrinkage of the lattice as they substitute indium sites in the cell. Even more significant is the fact that the linear dependence of the lattice spacing with gallium concentration implied that homogeneous $\text{CuIn}_{1-x}\text{Ga}_x\text{Se}_2$ alloys were produced for values of x between 0 and 0.35. According to Vegard's law there is a linear relationship in single-phase alloys between the lattice parameters and film composition.

3.3. Optical properties of the $\text{Cu}(\text{In}_{1-x}\text{Ga}_x)\text{Se}_2$ thin films

3.3.1 PL properties

The PL spectra for the $\text{Cu}(\text{In}_{1-x}\text{Ga}_x)\text{Se}_2$ layers are presented in Fig. 3. These measurements were conducted at 77K, and the broad band's suggest a donor–acceptor pair recombination, probably involving a copper vacancy (V_{Cu}) as acceptor and indium or gallium on copper site (In_{Cu} , Ga_{Cu}) as donor, as the material is slightly In-rich. The PL response of device quality slightly In-rich $\text{Cu}(\text{In}_{1-x}\text{Ga}_x)\text{Se}_2$ is known to be dominated by a broad donor–acceptor pair transition at approximately 0.950, 1.02 and 1.16 eV. The expected increase in peak position in the PL responses, with increase in gallium content, can clearly be seen. Another significant observation is the fact that the width (0.95, 0.114 and 0.118 eV) of the peaks also increases with an increase in gallium content. The sample containing the largest amount of gallium ($x = 0.35$) shows a weak second broad band at around 1.29 eV, which might be due to the intrinsic material properties caused by the increased substitution of indium by gallium. In order to estimate the band-gap energy, the binding energy of free excitons must be added to the energy position of the highest intensity line in the PL spectra, as indicated in Fig. 3. The values used for the binding energies for free excitons in CuGaSe_2 (14 meV) and CuInSe_2 (7.5 meV) have been determined and reported elsewhere [16, 17], and the binding energies of the $\text{Cu}(\text{In}_{1-x}\text{Ga}_x)\text{Se}_2$ structures in our study were calculated using the linear dependence on x . These calculated band energies are estimated values, as they actually represent a value that is slightly lower than the true band-gap energy. All these results are summarized in Table 1.

3.3.2 UV spectroscopy

In order to determine and confirm the band gap of the films in this study, optical transmission and reflectance measurements were conducted in the wavelength range between 300 and 2000 nm. The relationship between the optical absorption coefficient (α) and the incident photon energy ($h\nu$) from the optical absorption measurements for a direct band-gap material is given by

$$(\alpha h\nu)^2 \sim (h\nu - E_g) \quad (1)$$

Using this information, graphs of $(\alpha h\nu)^2$ were plotted against $h\nu$ and the linear region was extrapolated to $(\alpha h\nu)^2 = 0$ to give a value of the optical energy gap. The experimental optical band gap values for layers with varying gallium content (i.e. $x=0.02$, 0.22 and 0.35) were found to be approximately 1.02 , 1.08 and 1.21 eV, respectively. Fig. 4 displays the band-gap variation of the CGS layer as a function of gallium concentrations.

3.4. In-depth compositional uniformity of homogeneous $\text{Cu}(\text{In},\text{Ga})\text{Se}_2$ thin films

Figure 5 shows the in-depth compositional profiles of a typical homogeneous $\text{Cu}(\text{In}_{0.65}\text{Ga}_{0.35})\text{Se}_2$ film with a $\text{Ga}/(\text{Ga} + \text{In})$ atomic ratio of approximately 0.35 . The XPS depth profile results should be considered within the known limitation associated with depth profiling techniques using ion beam sputtering [18]. Against this background, it should be realized that the XPS results do not represent the exact compositional features of the compound, but are rather an indication of the distribution behavior of the elements in the bulk of the film. In this regard it is important to note that the concentration profiles of all the elements remained virtually constant in the region where the Mo signal was zero and decreased as soon as the Mo signal became significant. An exceptionally higher content of gallium at the surface and the bottom of the film, with a complementary low content value in indium peak, signifies that gallium was substituted for indium in the crystal structure. The homogeneous nature of the quaternary alloys prepared in the present study partly agree with those chalcopyrite deposited by standard two-step processes, which exhibit an accumulation of Ga towards the Mo back contact [5-10]. The relatively constant $\text{Ga}/(\text{Ga} + \text{In})$ ratios in these films are in agreement with XRD results, indicating virtually no variation in d-spacing through the entire depth of the absorber films. The profile does not show any presence of oxygen signifying the absence of oxides of In, Ga and Cu in the film. As seen in figure 5, no amount of silicon diffused into the film from the substrate.

4. Conclusions

Systematic structural, morphological, compositional and optical measurements, such as UV and PL spectroscopy dependence on the amount of gallium incorporation, were carried out on high-quality $\text{Cu}(\text{In}_{1-x}\text{Ga}_x)\text{Se}_2$ polycrystalline thin films. It is demonstrated that the combination of controlled growth conditions delivers single-phase $\text{Cu}(\text{In},\text{Ga})\text{Se}_2$ films with a high degree of in-depth compositional uniformity. This was nicely highlighted by the XRD spectrum showing all CIGS peaks, with shifts, indicating films with different gallium incorporations. CIGS peaks shifted to higher 2θ values than CIS due to a decrease in the lattice constant and increase in band-gap of the materials. Optical studies also indicated an increase in band-gap with increasing Ga content, confirming the homogeneous incorporation of Ga into the chalcopyrite lattice. These results were supported by SXPS, revealing a uniform distribution of the elements through the entire depth of the alloy. The production of homogeneous $\text{Cu}(\text{In},\text{Ga})\text{Se}_2$ chalcopyrite thin films with tunable lattice parameters and band-gap values is an important prerequisite for fabricating high-efficiency solar cell devices. This gives clear evidence that CIGS products will be important contenders on the PV power market.

Acknowledgments

The financial support of the National Research Foundation (Project No FA2006032700007) and University of the Free State is acknowledged. X-ray photoelectron spectroscopy work by Martin van Staden and Werner Jordaan of CSIR microscopy group is also gratefully acknowledged. This work was done within the framework of the Associateship Scheme of the Abdus Salam International Centre for Theoretical Physics, Trieste, Italy.

References

- [1] V Alberts, J Titus and R W Birkmire, 2004, Material and device properties of single-phase Cu(In,Ga)(Se,S)₂ alloys prepared by selenization/sulfurization of metallic alloys, *Thin Solid Films* **451–452** 207
- [2] K Ramanathan, M A Contreras, B Egaas, J Hiltner, A Swartzlander, F Hasoon and R Noufi, Properties of 19.2% efficiency ZnO/CdS/CuInGaSe₂, 2003 *Prog. Photovolt., Res. Appl.* **11** 225
- [3] V Alberts, J H Schön and E Bucher, Improved material properties of polycrystalline CuInSe₂ prepared by rapid thermal treatment of metallic alloys in H₂Se/Ar, 1998 *J. Appl. Phys.* **84** 6881
- [4] B Basol, V J Kapur, C R Leidholm, A Halani and K Gledhill, Flexible and light weight copper indium diselenide solar cells on polyimide substrates, 1996 *Sol. Energy Mater. Sol. Cells* **43** 93
- [5] M Marudachalam, R W Birkmire, H Hichri and J M Schultz, Phases, morphology, and diffusion in CuIn_xGa_{1-x}Se₂ thin films, 1997 *J. Appl. Phys.* **82** 2896
- [6] M. Marudachalam, H. Hichri, R. Klenk, R. Birkmire, W. Shafarman, and J. Schultz, Preparation of homogeneous Cu(InGa)Se₂ films by selenization of metal precursors in H₂Se atmosphere, *Appl. Phys. Lett.* **67**, 3978 (1995)
- [7] B. M. Basol, V. K. Kapur, A. Halani, C. R. Leidholm, J. Sharp, J. R. Sites, A. Swartzlander, R. Matson, and H. Ullal, Cu(In,Ga)Se₂ thin films and solar cells prepared by selenization of metallic precursors, *J. Vac. Sci. Technol. A* **14**, 2251 (1996)
- [8] M. Marudachalam, R. W. Birkmire, H. Hichri, J. M. Schultz, A. Swartzlander, and M. M. Al-Jassim, Phases, morphology, and diffusion in CuIn_xGa_{1-x}Se₂ thin films, *J. Appl. Phys.* **82**, 2896 (1997)
- [9] T Nakada, H Ohbo, T Wanatabe, H Nakazawa, M Matsui and A Kunioka, Improved Cu(In,Ga)(S,Se)₂ thin film solar cells by surface sulfurization, 1997 *Solar Energ. Mat. Sol. C.* **49** 285
- [10] Y Nagoya, K Kushiya, M Tachiyuki and O Yamase, Role of incorporated sulfur into the surface of Cu(InGa)Se₂ thin-film absorber, 2001 *Sol. Energ. Mat. Sol. C.* **67** 247

- [11] J Palm, V Probst, W Stetter, R Toelle, S Visbeck, H Calwer, T Niesen, H Vogt, O Hernandez, M Wendl and F H Karg, CIGSSe thin film PV modules: from fundamental investigations to advanced performance and stability, 2004 Thin Solid Films 451–452 544
- [12] V Alberts, S Zweigart and H W Schock, Preparation of device quality CuInSe₂ by selenization of Se containing precursors in H₂Se atmosphere Semiconductor Science and Technology, 1997 Semicond. Sci. Technol. 12 217
- [13] Arya R., Lommasson T., Wied Man S., Russell L., Skibo S. and Fogleboch J., JEEEC, pp. 516-520, (1993)
- [14] Al Bassam A., Mater. Chem. Phys. 53, p. 1-5, (1998)
- [15] R Pal, K K Chattopadhyay, S Chaudhuri and A K Pal, Variation of trap state density and barrier height with Cu/In ratio in CuInSe₂ films, Thin Solid Films 247 pp. 8-14, (1994).
- [16] S. Chichibu, T. Mizutani, K. Murakami, T. Shioda, T. Kurafuji, H. Hakanishi, P.J. Fons, S. Niki, A. Yamada, Band gap energies of bulk, thin-film and epitaxial layers of CuInSe₂ and CuGaSe₂, Journal of Applied Physics 83 (1998) 3678–3689
- [17] A. Meeder, D. Fuertes Marron, V. Chu, J. P. Conde, A. Jager -Waldau, A. Rumberg, M. Ch. Lux-Steiner, Photoluminescence and sub band gap absorption of CuGaSe₂ thin films, Thin Solid Films 403–404 (2002) 495–499
- [18] A Galdikas and L Pranevicius, Surface composition changes of ternary alloys in the non-steady state regime of preferential sputtering, 2000 Nucl. Instrum. Methods B 164–165 868

Table 1: Increase in calculated and experimental band-gap energy with increase in gallium content for $\text{Cu}(\text{In}_{1-x}\text{Ga}_x)\text{Se}_2$ alloys.

Structure	Calculated BE (meV)	Energy from PL (eV)	Estimated band gap (eV)	Experimental band gap (eV)
$\text{CuIn}_{0.98}\text{Ga}_{0.02}\text{Se}_2$	7.6	0.95	0.96	1.01
$\text{CuIn}_{0.78}\text{Ga}_{0.22}\text{Se}_2$	8.9	1.02	1.03	1.08
$\text{CuIn}_{0.65}\text{Ga}_{0.35}\text{Se}_2$	9.8	1.16	1.17	1.21

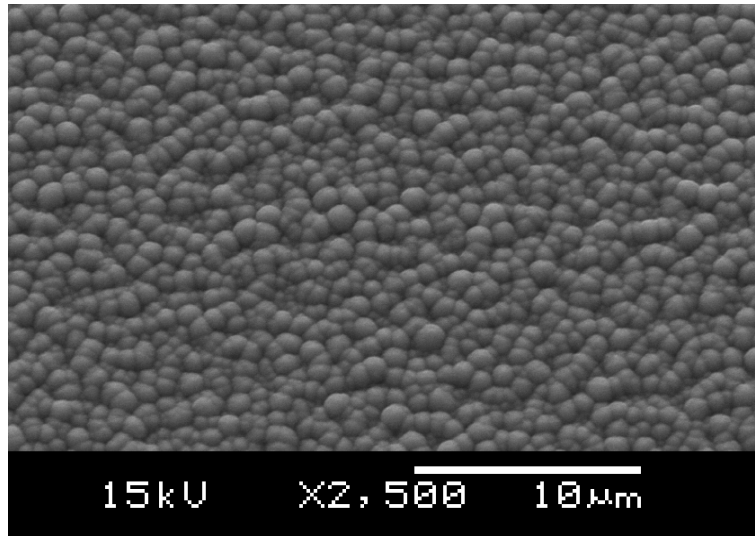


Figure 1(a): The SEM pattern of the structural features of the precursor structure deposited at 200 °C.

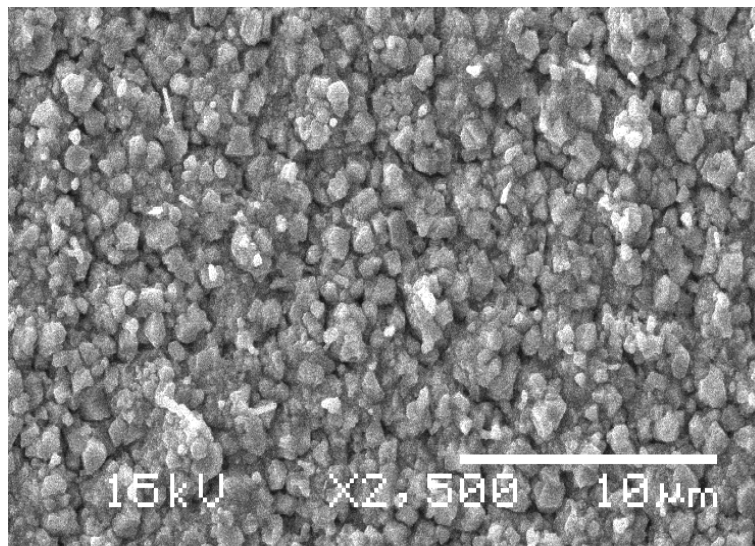


Figure 1(b): SEM micrographs showing the morphological features of a fully reacted Cu(In,Ga)Se_2 film. Selenization was conducted in elemental Se vapour at 550 °C for 60 min.

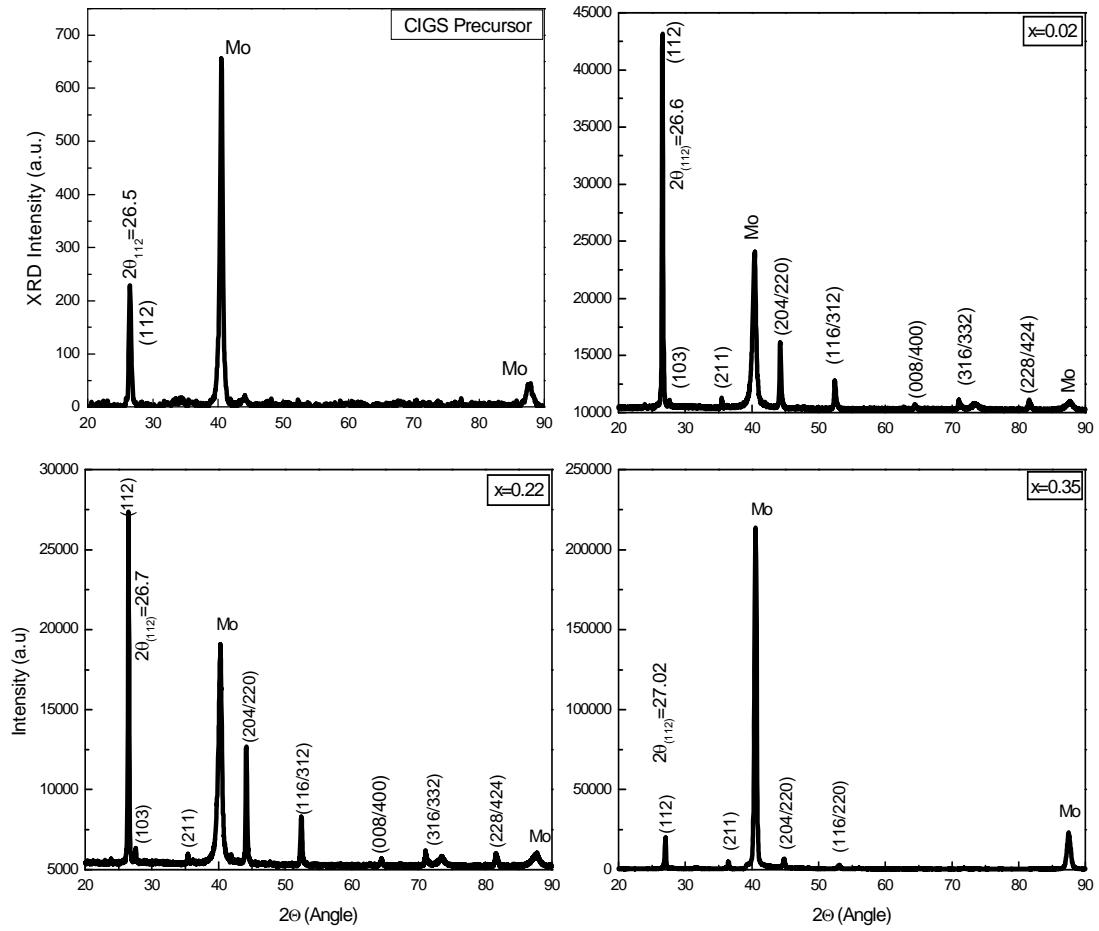


Figure 2(a): XRD patterns of the precursor and $\text{CuIn}_{1-x}\text{Ga}_x\text{Se}_2$ selenized thin films with different gallium incorporations ($x=0.02, 0.22$ and 0.35).

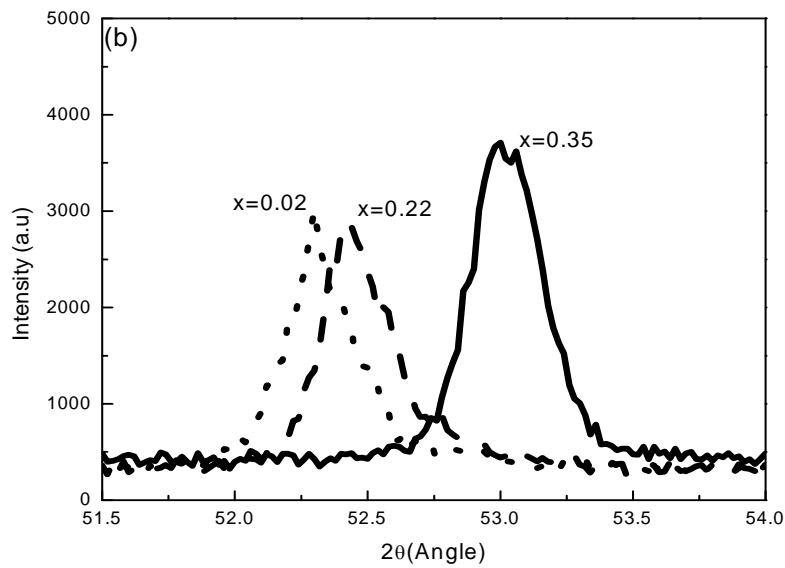


Figure 2(b): Position of the [116/312] diffraction peaks of single-phase $\text{CuIn}_{1-x}\text{Ga}_x\text{Se}_2$ as function of gallium concentration ($x=0.02, 0.22$ and 0.35).

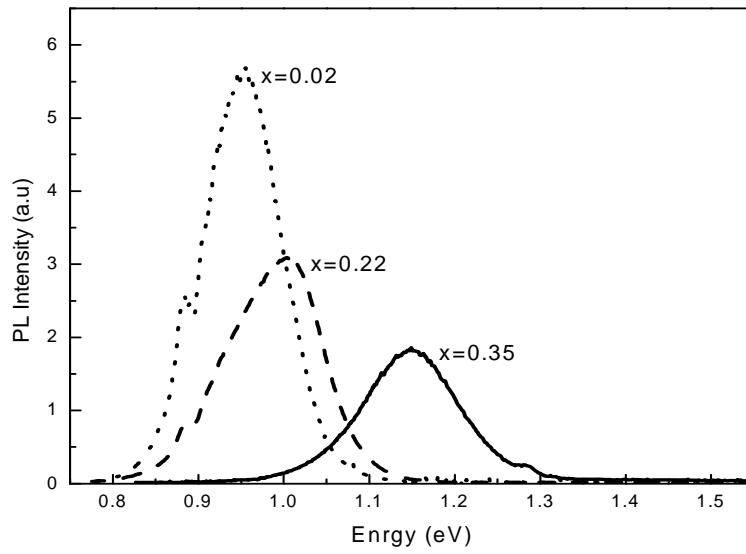


Figure 3: PL spectra for $\text{CuIn}_{1-x}\text{Ga}_x\text{Se}_2$ samples selenized at $550\text{ }^\circ\text{C}$ for 60 min, for different gallium concentration ($x=0.02, 0.22$ and 0.35). Measurements were conducted at 77K , using a 5mW laser at an excitation wavelength of 514.5 nm . The increase of the broadband peak position with increasing gallium content (increase in x) is observed.

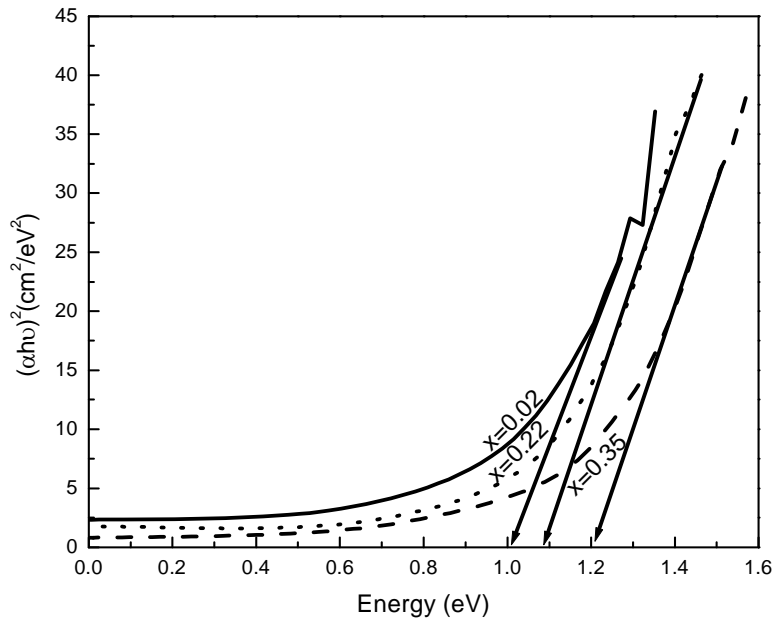


Figure 4: Graph of $(\alpha h\nu)^2$ vs $h\nu$ for different concentrations of gallium in $\text{CuIn}_{1-x}\text{Ga}_x\text{Se}_2$ absorbers.

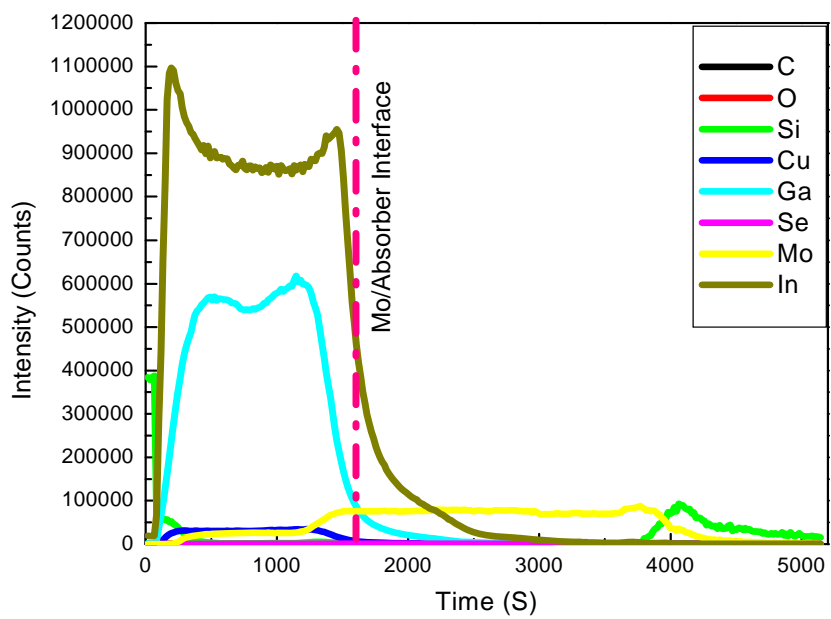


Figure 5: XPS depth profile for a single-phase $\text{CuIn}_{1-x}\text{Ga}_x\text{Se}_2$ sample, clearly depicting the uniform distribution of the respective elements in the alloy.